Dyes and Pigments 131 (2016) 206–214

Contents lists available at ScienceDirect

Dyes and Pigments

journal homepage: www.elsevier.com/locate/dyepig

Multistep assembling *via* intermolecular interaction between (bis) styryl dye and cucurbit[7]uril: Spectral effects and host sliding motion

Ekaterina Y. Chernikova [a, *], Sergey V. Tkachenko [a], Olga A. Fedorova [a, b], Alexander S. Peregudov [a], Ivan A. Godovikov [a], Nikolay E. Shepel [a], Stela Minkovska [c], Atanas Kurutos [d], Nikolay Gadjev [d], Todor G. Deligeorgiev [d], Yuri V. Fedorov [a]

[a] A.N. Nesmeyanov Institute of Organoelement Compounds of Russian Academy of Sciences, Vavilova St., 28, 119991 Moscow, Russia
[b] D. Mendeleyev University of Chemical Technology of Russia, Miusskaya Sq., 9, 125047 Moscow, Russia
[c] Institute of Catalysis Bulgarian Academy of Sciences, Acad. G. Bonchev St., Bldg. 11, Sofia 1113, Bulgaria
[d] Faculty of Chemistry and Pharmacy, Sofia University "St. Kliment Ohridski", 1, Blv. J. Bourchier, 1164 Sofia, Bulgaria

ARTICLE INFO

Article history:
Received 21 January 2016
Received in revised form
4 April 2016
Accepted 6 April 2016
Available online 7 April 2016

Keywords:
Cucurbit[7]uril
(Bis)styryl dye
Supramolecular chemistry
Host–guest complex
Protonation
Molecular shuttle

ABSTRACT

The host–guest interaction between bis(styryl)pyridinium dye (**BSP**) and cucurbit[7]uril (CB[7]) was studied by means of optical spectroscopy, ^{1}H and 2D (COSY, ROESY, DOSY) NMR spectroscopy and electrospray ionization mass spectrometry in different microenvironment (aqueous or phosphate buffer solution). The CB[7] macrocycles bind to **BSP** dye in a stepwise manner thus forming higher stoichiometric complexes such as $(H^+)_2$–**BSP**–$(CB[7])_3$ in aqueous or **BSP**–$(CB[7])_3$ in buffered solution. In the case of aqueous solution, complex formation is accompanied by the host-assisting protonation of the anilino-type **BSP** nitrogen atoms, that causes a pronounced effect on its spectral properties. Stimuli-responsive sliding movements of the CB[7] macrocycles along the stalk of dye molecule were also observed.

1. Introduction

Nowadays, bischromophoric styryl dyes receive growing attention due to their useful properties providing versatile applications in technology, science and medicine. Specifically, these molecules have been used in organic electronics (e.g., OLED devices) and photonics, optical storage and recording systems, three-dimensional (3D) lithography, nonlinear optical materials, dye lasers, molecular sensors, logic gates and fluorescent labeling for the visualization of biological objects [1–8]. The effective strategy to modify and improve the intrinsic molecular properties of dyes is the use of non-covalent supramolecular interactions *via* formation of the host–guest assemblies with macrocyclic molecules [9,10].

Cucurbit[*n*]urils (CB[*n*], where *n* is most commonly 5–8) are water soluble macrocyclic host molecules comprising two identical ureidyl carbonyl portals with high negative charge density and rigid extremely non-polarizable (close to gas phase) inner cavity [11–14]. Owing to their unique structure, CB[*n*]s exhibit high tendency to form stable inclusion complexes of different stoichiometries with positively charged organic molecules due to ion-dipole and hydrophobic interactions [15–17]. The effects of CB[*n*] encapsulation on the molecular properties of the chromophoric guest molecules, such as dyes and fluorophores, have been the subject of several research groups. Detailed experimental study of supramolecular host–guest assemblies were performed for various derivatives of xanthene, coumarin, oxazine, cyanine, diazine, acridine, triphenylmethane, naphthalimide, anthraquinone and porphyrin in aqueous solution [18–32]. Inclusion of chromophoric guests into the CB[*n*] cavity usually gives rise to the increased fluorescence intensity, prolongation of the fluorescence lifetimes, improved brightness, shifting of spectral (absorption and fluorescence) band and reducing of Stokes shift [33–36]. For example, the most dramatic ~1700-fold enhancement in the emission intensity was observed by J. Mohanty and A. C. Bhasikuttan for thiazole orange upon adding CB[8] [37]. CB[*n*] participates in the modification of

* Corresponding author. Laboratory of Photoactive Supramolecular Systems, A.N. Nesmeyanov Institute of Organoelement Compounds of Russian Academy of Science, Vavilova St., 28, 119991 Moscow, Russia.
E-mail address: chernikova@ineos.ac.ru (E.Y. Chernikova).

http://dx.doi.org/10.1016/j.dyepig.2016.04.013
0143-7208/

the excited-state properties of guest molecules. In particular, CB[7] can disrupt twisted intramolecular charge transfer (TICT) [24,38,39] and photoinduced electron transfer (PET) [40,41] processes in photoexcited dye molecules, thus significantly improving their fluorescence response. Control over the excited state proton transfer (ESPT) reaction has been achieved through encapsulation of hydroxyphenyl benzimidazole by CB[7] [42,43]. Moreover, W. M. Nau and J. Mohanty have demonstrated that CB[7] can act as a cation receptor, causing a remarkable shift in the protolytic equilibria (p*Ka* up to 5.2 units) and stabilizing the protonated form of chromophoric guest molecules [44–46]. Thermal and photochemical stability, solubility in aqueous solutions [18,34,47], protection against molecular aggregation [48–52] are practical features of dyes, which can be improved and effectively managed by complex formation with CB[7] as well. CB[*n*]-induced changes of the molecular properties of guest molecules in the ground and excited states have been introduced into a number of advantageous applications including design and synthesis of fluorescent sensors and on/off switches, photofunctional materials such as logic gates, light-resistant materials, stabilizing additives for laser dyes, drug delivery systems and other functional assemblies [53–58].

Contributing to this area, we have explored the increased binding affinity of CB[7] towards cationic chromophoric guests to alter spectral and photophysical properties of bis(styryl)pyridinium dye (**BSP**) in aqueous solution. **BSP** molecule consists of two dimethylamino 4-styryl(pyridinium) moieties linked by tetramethylpropandiamino unit that provides formation of symmetrical and multicharged structure, as sketched in Chart 1. In our recent study [22], we have demonstrated that dicationic bis(styryl) dyes bearing short nonpolar linking groups undergo encapsulation by CB [7] that result in formation of complexes with linear or/and folded structures. Unlike the previously studied dyes, new **BSP** dye possesses a positively charged spacer which provides additional binding site for CB[7].

2. Materials and methods

Cucurbit[7]uril was synthesized according to known procedures [59,60]. (E)-1,1'-((propane-1,3-diylbis(dimethylammonionediyl)) bis(propane-3,1-diyl))bis(4-((E)-4-(dimethylamino)styryl)pyridin-1-ium) iodide (**BSP**) was obtained according to the described in the literature method [61]. All solvents and other reagents are commercial products (Sigma Aldrich, TCI Europe) and were used without further purification. Preparation of the dye solutions and all experiments were carried out in a laboratory environment of red light. Deionized water (Milli-Q) was employed for all aqueous solutions. Phosphate buffer solution (Na_2HPO_4/NaH_2PO_4 with pH = 7.00 (10 mM)) was used to maintain a constant pH value of aqueous solution of **BSP** in the presence of CB[7].

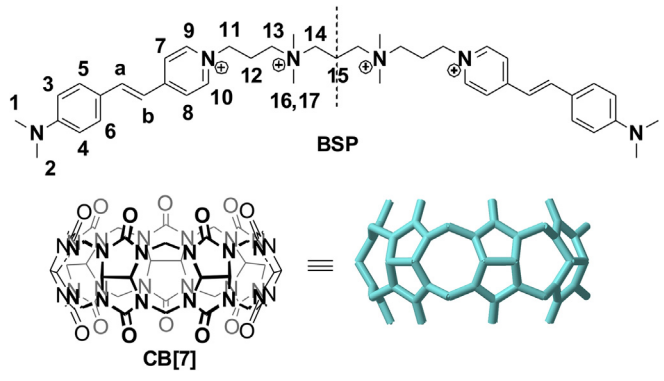

Chart 1. Chemical structures of cucurbit[7]uril (CB[7]) and bis(styryl)pyridinium dye (**BSP**).

The NMR experiments were carried out in D_2O using a Bruker Avance™ spectrometers operating at 500 and 600 MHz. The spectrometers were equipped with an inverse gradient probe-head. All ^1H as well as 2D experiments (COSY, ROESY, DOSY) were performed at 298 K using standard pulse sequences from the Bruker library. ^1H chemical shifts were determined with an accuracy of 0.01 ppm and are given relative to the residual signal of the solvent that was used as internal reference. Spin–spin coupling constants were determined with accuracy of 0.1 Hz.

The absorption spectra measurements were performed using a Varian-Cary 100 spectrophotometer (1 cm quartz cell). The fluorescence spectra measurements were performed using a FluoroLog-3 Model FL3-221 (Jobin Yvon) spectrofluorimeter. The fluorescence quantum yield measurements were performed using Varian-Cary 100 spectrophotometer and a FluoroLog-3 spectrofluorimeter. All measured fluorescence spectra were corrected for the nonuniformity of detector spectral sensitivity. Rhodamine 6G in ethanol ($\Phi_{fl} = 0.95$, [62]) was used as a reference for the fluorescence quantum yield measurements.

Electrospray ionization mass spectrometry (ESI-MS) analyses were performed using a Finnigan LCQ Advantage mass spectrometer equipped with an octopole ion-trap mass-analyzer, an MS Surveyor pump, a Surveyor auto sampler, a Schmidlin-Lab nitrogen generator (Germany), and Finnigan X-Calibur 1.3 software for data collecting and processing. Direct infusion of the sample solution was used. Positive electrospray ionization was achieved using an ionization voltage at 4 kV at temperature of 200 °C. Electrospray full scan spectra in the range *m/z* 100–2000 were obtained by infusion at 0.05 mL min^{-1} of 25 μM aqueous solutions of **BSP** alone or in the presence of 1, 2 or 5 equiv. of CB[7].

Complex formation of dye **BSP** with CB[7] in H_2O + CH_3CN (1–2%) at 20 ± 1 °C was studied by spectrophotometric titration. The ratio of dye **BSP** to CB[7] was varied by adding aliquots of a solution containing known concentrations of **BSP** and CB[7] to a solution of **BSP** alone of the same concentration. The absorption spectrum of each solution was recorded and the stability constants of the complexes were determined using the «SPECFIT/32» program (Spectrum Software Associates, PMB 361, 197M Boston Post Road, West Marlborough, MA 01752, U.S.A.). Interactions between **BSP** with CB[7] in buffer solution and protonation of **BSP** by $HClO_4$ were also studied by the same method.

3. Results and discussion

3.1. Optical spectra study

The traditional way to shift the protolytic equilibrium of pH-sensitive molecules is its immersion in acidic environment. Recently, different research groups have established that supramolecular encapsulation by CB[7] resulted in pronounced pK_a shifts of the chromophoric molecules due to different affinity of the host to the protonated and neutral guests [44–46]. The UV/Vis spectrum of **BSP** in aqueous solution is characterized by a very intense long wavelength absorption band centered at 482 nm ($\varepsilon = 5.99 \times 10^4$ M^{-1} cm^{-1}), as illustrated in Fig. 1a. This band is assigned to an efficient intramolecular charge transfer (ICT) process from donor dimethylamino groups to acceptor pyridinium rings. We started our research with the study of dye protonation upon addition of perchloric acid to the **BSP** in aqueous solution. On gradual increase of the $HClO_4$ concentration in the solution of the free dye, the absorption maximum undergoes pronounced hypsochromic shift from 482 to 335 nm (Fig. S2). Analysis of the spectra obtained from spectrophotometric titration provided the two

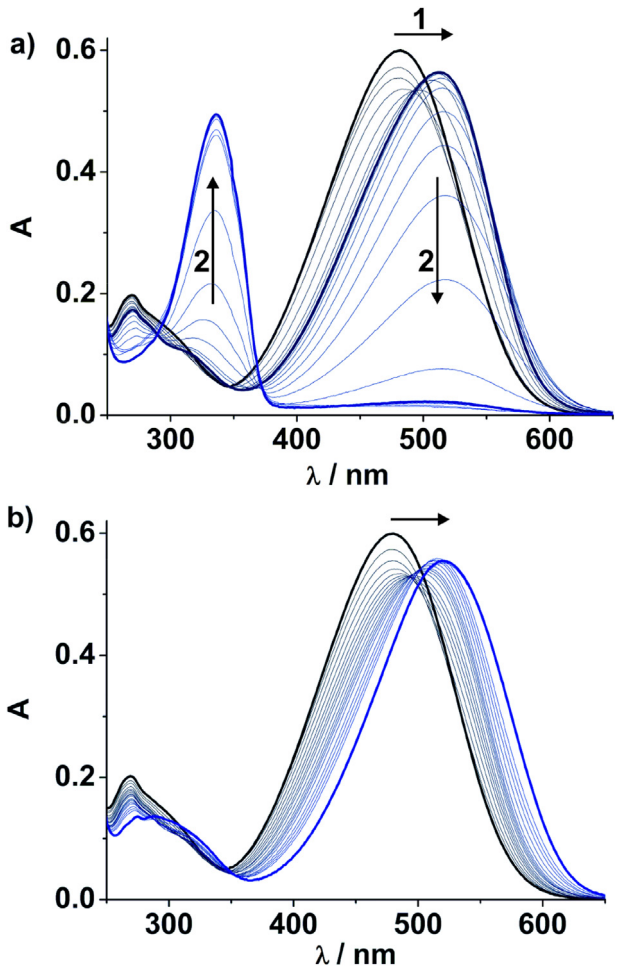

Fig. 1. UV–Vis spectra of **BSP** (1.0×10^{-5} M) a) with increasing CB[7] concentration ($0 \div 6.7 \times 10^{-4}$ M) in H_2O; b) with increasing CB[7] concentration ($0 \div 1.0 \times 10^{-3}$ M) in phosphate buffered solution (Na_2HPO_4/NaH_2PO_4) at pH = 7.00.

association constants for the mono- ($\log K_{11} = 3.21 \pm 0.06$) and di-protonated ($\log K_{12} = 5.96 \pm 0.09$) dye (Fig. S3). Next, we evaluated the UV/Vis spectral changes of **BSP** in the presence of CB[7] in aqueous solution. The incremental addition of CB[7] to a solution of **BSP** (10 μM) up to about 3 equiv. initially results in a moderate bathochromic shift ($\Delta\lambda_{max} = 32$ nm) of the absorption band up to 514 nm, which is diagnostic for inclusion of dye in a less polar environment. Further increase of the amount of CB[7] up to about 40 equiv. causes a new blue-shifted band at 336 nm to appear and the band at 514 nm to disappear simultaneously (Fig. 1a). Such a large 146 nm hypsochromic shift of long wavelength absorption band of the free dye on complex formation with CB[7] results in easily observed complete discoloration of initially brick red solution. Apparently, noncovalent host–guest interactions which connect dye molecules to CB[7] cannot have such a notable influence on absorption spectra, leading to blockage of ICT process. The most obvious explanation of the observed experimental facts arises from the strong modulation of the molecular structure of **BSP**, namely, protonation of donor dimethylamino groups at the sufficient excess of CB[7].

We attempted to determine the stoichiometry and association constants of host–guest complexes of CB[7] with **BSP** by analyzing the set of corresponding spectrophotometric titration data (Fig. 1a). However, we faced the problem, which most likely can be attributed to the formation of mono- and di-protonated forms of **BSP** at high (5–67 equiv.) excess of CB[7]. It results in formation of multicomponent solution during titration preventing the determination of the stoichiometry and association constants of the complexes with enough reliability. So, unfortunately, despite the calculated association constants of **BSP** with perchloric acid (see below), we failed to determine the stoichiometry and association constants of the complexes from the total set of spectrophotometric titration data. At the same time we succeeded in association constants determination at low concentration of CB[7] (up to 3 equiv.), where the influence of the dye protonation is neglected. The one-to-one and one-to-two stoichiometry for host–guest complexes can be deduced from the partial titration curve (Fig. S1a). The association constants of complexes **BSP**–CB[7] and **BSP**–$(CB[7])_2$ ($\log K_{11} = 6.4 \pm 0.4$ and $\log K_{12} = 11.9 \pm 0.3$) and their absorption spectra were obtained by a global fit of the spectrophotometric titration data using the SpecFit/32 program (Table S1 and Fig. 2a). These equilibrium constants correspond to binding of one or two CB[7] molecules with unprotonated **BSP** molecule.

To exclude the influence of protonation of **BSP** on complex formation with CB[7], spectrophotometric titration in the phosphate buffer solution (Na_2HPO_4/NaH_2PO_4, 10 mM) at pH = 7.00 was carried out. The addition of CB[7] to a solution of **BSP** resulted in a moderate bathochromic shift ($\Delta\lambda_{max} = 38$ nm) of the long wavelength absorption band as it was observed for the similar styryl dyes earlier [22]. At the same time the short-wavelength absorption band at 336 nm is not appeared because there is no

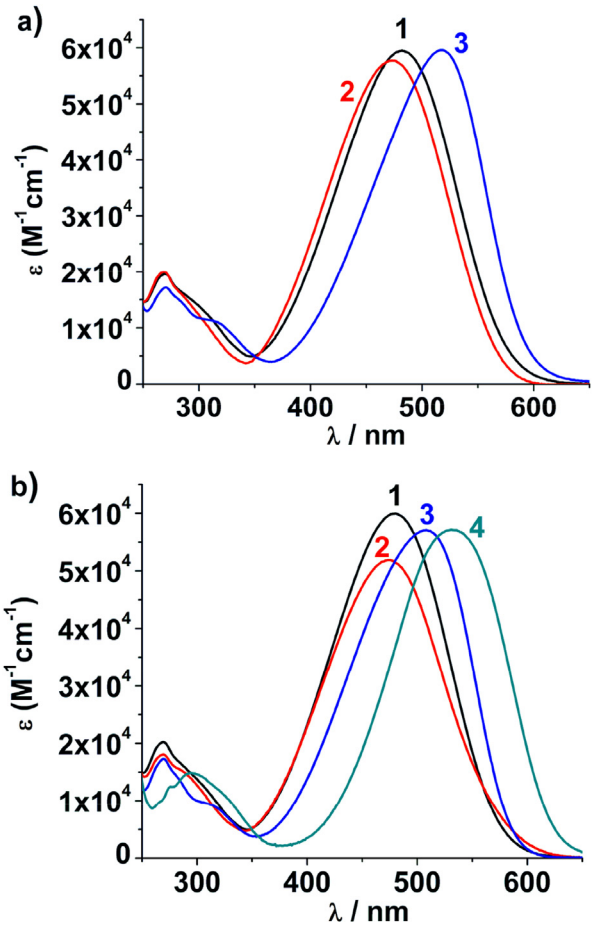

Fig. 2. Electronic absorption spectra obtained by a global fit of the spectrophotometric titration data using the SpecFit/32 program for a) **BSP** (1) and its complexes **BSP**–CB[7] (2) and **BSP**–$(CB[7])_2$ (3) in H_2O; b) **BSP** (1) and its complexes **BSP**–CB[7] (2), **BSP**–$(CB[7])_2$ (3) and **BSP**–$(CB[7])_3$ (4) in phosphate buffer solution.

protonation of **BSP** at pH 7. The set of spectrophotometric titration curves (Fig. 1b) was analyzed using Specfit/32 software in order to determine the association constants of host–guest complexes. Three equilibria were considered in the fitting:

$$L + M \overset{K_{11}}{\rightleftharpoons} LM,\ K_{11} = \frac{[LM]}{[L]\cdot[M]}$$

$$L + 2M \overset{K_{12}}{\rightleftharpoons} LM_2,\ K_{12} = \frac{[LM_2]}{[M]^2\cdot[L]}$$

$$L + 3M \overset{K_{13}}{\rightleftharpoons} LM_3,\ K_{13} = \frac{[LM_3]}{[L]\cdot[M]^3}$$

where L and M stand for the free dye and host, respectively, LM, LM_2 and LM_3 stand for dye–host complexes and K_{11}, K_{12}, K_{13} are the association constants.

The spectral set for **BSP** and CB[7] in phosphate buffer at pH = 7.00 is consistent with formation of three complexes having 1:1, 1:2 and 1:3 stoichiometries, namely, **BSP**–CB[7], **BSP**–$(CB[7])_2$ and **BSP**–$(CB[7])_3$, with association constants equal to $\log K_{11} = 5.4 \pm 0.4$, $\log K_{12} = 10.4 \pm 0.3$ and $\log K_{13} = 14.0 \pm 0.2$ correspondingly. Electronic absorption spectra of these complexes obtained by a global fit of the spectrophotometric titration data using the SpecFit/32 software are shown in Fig. 2b. The absorption spectra of **BSP**–CB[7] and **BSP**–$(CB[7])_2$ complexes in phosphate buffer and in the aqueous solution are practically the same (Fig. 2a). The long wavelength absorption band of **BSP**–CB[7] complex is slightly blue-shifted relative to the absorption band of the free dye by 9 or 5 nm (in aqueous or buffer solution, respectively), while the absorption band of **BSP**–$(CB[7])_2$ complex is red-shifted relative to absorption of the free dye by about 36 or 27 nm (in aqueous or buffer solution, respectively). These findings indicate that host–guest interactions in the complexes of identical stoichiometry discussed here are quite similar. We should also notice that the association constants of **BSP**–CB[7] and **BSP**–$(CB[7])_2$ complexes in aqueous solution are higher than in phosphate buffer (Table S1). A slight reduction of the association constants of these complexes in the buffer solution is in accordance with the well-known ability of CB[7] to act as ionophore for metal cations in aqueous solution due to interaction of metal cations with the carbonyl portals of CB[7] ($K_{CB[7]Na+}$ = 80-120 M^{-1}, [63,64]). Examples of similar variations of the association constants of incorporated guests can be found in the literature [25,65–67].

The relevant fluorescence characteristics were also obtained for **BSP** + CB[7] system in the aqueous as well as phosphate buffer solution (see ESI). Complicated changes in the emission spectra of **BSP** on complex formation with CB[7] were found (Fig. S6).

3.2. NMR spectra study

To get insight into the structure of host–guest complexes, ^{1}H NMR measurements of **BSP** upon adding of growing amount of CB[7] were performed. The ^{1}H NMR assignments were ascertained by 2D NMR techniques including ROESY and COSY (Figs. S9–S32). By careful analysis of the ^{1}H NMR spectrum of **BSP** in the presence of 0.5 equiv. of CB[7] in D_2O, we found that resonances for all protons are slightly downfield shifted by about 0.04–0.08 ppm (marked in pink color in Fig. 3a). The same proton resonances (by 0.03–0.06 ppm) of **BSP** were found in the presence of 1 equiv. of CB[7]. In both cases no any shielding effect of hydrophobic cavity of CB[7] was observed for protons of dye molecule. Based on the NMR observation we propose the structure of **BSP**–CB[7] complex as shown on Scheme 1 where the two styrylpyridinium moieties and tetramethyl propandiaminium linker of **BSP** are located outside the CB[7] cavity by folding of the aliphatic chain, similar to early reported complexes between CB[7] and bis(styryl) dyes [22]. Such exclusion complex is mainly stabilized by van der Waals intermolecular forces and ion-dipole interactions between electron-rich carbonyl oxygen atoms of CB[7] portals and pyridinium nitrogen atoms and quaternized nitrogen atoms of the central linker of **BSP**. The distance between four positively charged nitrogen atoms is too small to engulf alkyl fragments of linker into the cavity of CB[7]. So, most protons in the ^{1}H NMR spectrum of **BSP** fall under deshielding action of CB[7] cavity. The similar exclusion complexes have been found in literature [36,38].

Upon addition of a slight excess of CB[7] (1.5–2.5 equiv.) to the **BSP** solution, the pattern of complexation-induced chemical shifts is changed. The presence of 1.5 equiv. of CB[7] leads to a splitting of the guest proton resonances into three sets as a result of a slow exchange rate on the NMR time scale between all species (Fig. 3). The first set of signals is similar to those of the exclusion complex. This set of signals disappeared completely at the **BSP**/CB[7] molar ratio of 1:2. The other new sets of proton resonances are associated with the two different inclusive complexes similar to [3]pseudorotaxanes. Let us consider the second set of proton signals of **BSP** (marked in green color in Fig. 3). Compared to free dye, the resonances for ethylene fragments ($\Delta\delta H_a = -0.66$ ppm and $\Delta\delta H_b = -0.66$ ppm at 1:2 **BSP**/CB[7] ratio) and pyridinium rings ($\Delta\delta H_{7,8} = -0.37$ ppm and $\Delta\delta H_{9,10} = -0.28$ ppm at 1:2 **BSP**/CB[7] ratio) protons are dramatically shifted to higher field, indicating their inclusion into CB[7] cavity. Conversely, the aliphatic protons of linker ($\Delta\delta H_{11} = +0.16$ ppm at 1:2 **BSP**/CB[7] ratio) and aromatic protons ($\Delta\delta H_{3,4} = +0.39$ ppm and $\Delta\delta H_{5,6} = +0.36$ ppm at 1:2 **BSP**/CB[7] ratio) exhibit downfield shifts, showing their location just outside the CB[7] cavity. These findings clearly suggest that **BSP** molecule is encapsulated in the hydrophobic cavity of CB[7] with the formation of an inclusion complex **BSP**–$(CB[7])_2$. Taking into account the data reported [68], we assumed that CB[7] macrocycles in [3]pseudorotaxane are located over the aromatic part of **BSP**, close to the pyridinium groups, as illustrated on Scheme 1.

Inspection of the third set of proton resonances of **BSP** (marked in blue color in Fig. 3) indicates that signals assigned to the aromatic protons ($\Delta\delta H_{5,6} = -0.53$ ppm) and ethylene fragments protons ($\Delta\delta H_a = -0.18$ ppm and $\Delta\delta H_b = -0.45$ ppm at 1:2.5 **BSP**/CB[7] ratio) are significantly upfield shifted, whereas the signals of the pyridinium rings ($\Delta\delta H_{7,8} = +0.38$ ppm and $\Delta\delta H_{3,4} = +0.15$ ppm at 1:2.5 **BSP**/CB[7] ratio) undergo the deshielding effect of the carbonyl groups of CB[7]. At the same time, chemical shifts of the protons adjacent to dimethylammonium groups to the lower field region become more pronounced ($\Delta\delta H_{1,2} = +0.37$ ppm and $\Delta\delta H_{3,4} = +0.30$ ppm at 1:2.5 **BSP**/CB[7] ratio), supporting the concomitant protonation of aniline-type nitrogen atoms in the excess of CB[7]. The 2D-ROESY NMR spectra also displayed cross-peaks between pyridinium protons $H_{3,4}$ and $H_{5,6}$ and singlet at 3.08 ppm attributed to N–H protons on ammonium groups (along with singlet of $H_{1,2}$ protons for methyl groups at 3.20 ppm). Taken together, these facts reveal that the complex formed is [3]pseudorotaxane $(H^+)_2$–**BSP**–$(CB[7])_2$ where the CB[7] macrocycles reside over the phenylethelene moieties nearby dimethylamino groups with the pyridinium rings staying outside. Thus, the changes in chemical shifts of $(H^+)_2$–**BSP**–$(CB[7])_2$ complex would be due to a combination of following contributions: a) chemical shifts arising from a protonation of the guest molecule; b) CB[7]-induced chemical shifts in the 1:2 complex.

It is interesting that CB[7] in $(H^+)_2$–**BSP**–$(CB[7])_2$ complex slides away from the pyridinium ring and encircles the vicinity of dimethylamino groups, what is quite different from the location of CB[7] in **BSP**–$(CB[7])_2$ complex. Indeed, it is impossible for the two CB[7] macrocycles to surround the both sides of the pyridinium

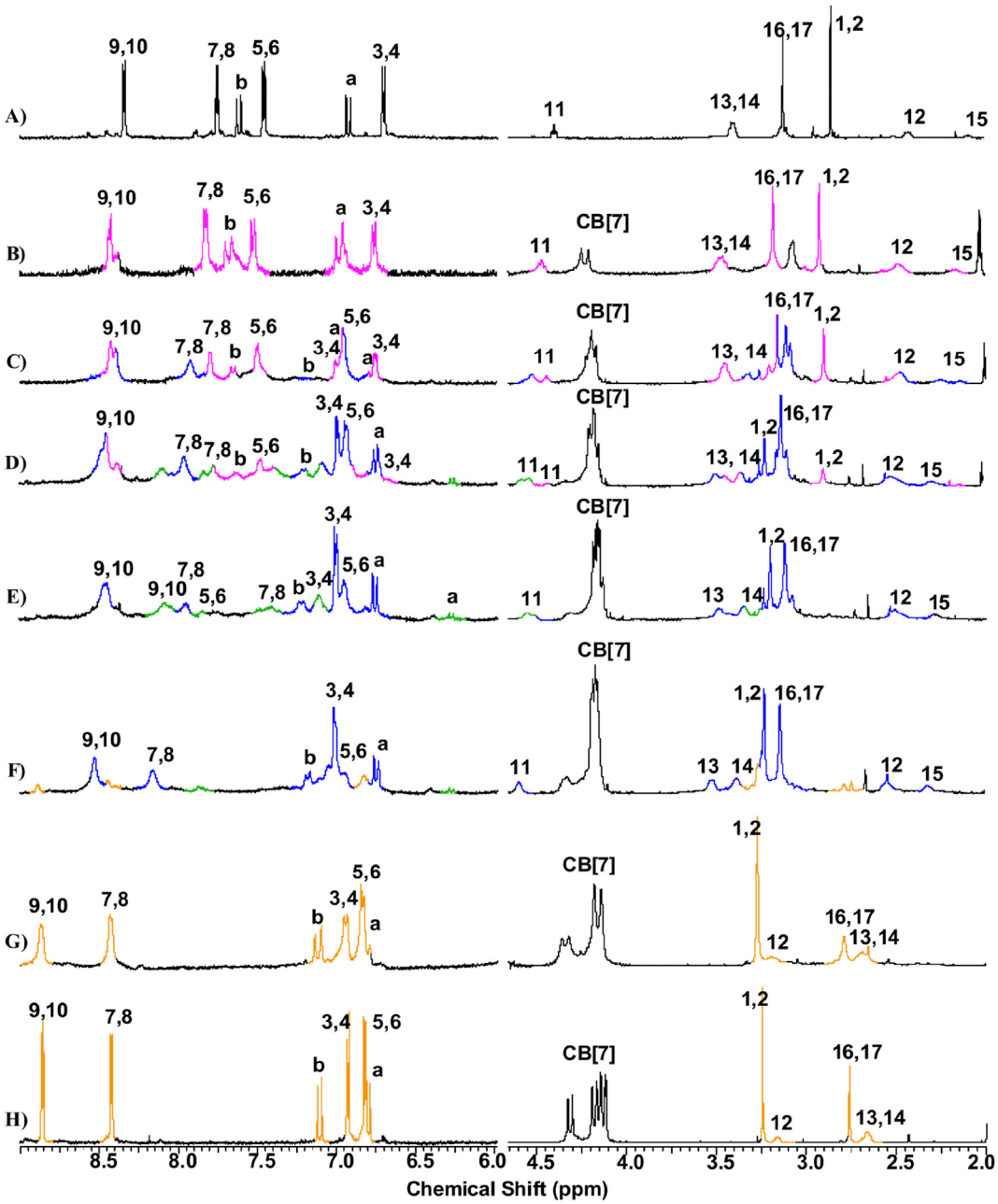

Fig. 3. ^{1}H NMR spectra recorded (600 MHz, 298 K, in D_2O) for (A) BSP (1.0 mM); (B) BSP·CB[7] (1.0 mM/0.5 mM); (C) BSP, CB[7] (1.0 mM/1.0 mM); (D) BSP, CB[7] (1.0 mM/1.5 mM); (E) BSP, CB[7] (1.0 mM/2.0 mM); (F) BSP, CB[7] (1.0 mM/2.5 mM); (G) BSP, CB[7] (1.0 mM/3.5 mM); (H) BSP, CB[7] (1.0 mM/5.0 mM). Color code: free BSP, black; **BSP**–CB[7], pink; **BSP**–$(CB[7])_2$, green; $(H^+)_2$–**BSP**–$(CB[7])_2$, dark blue; $(H^+)_2$–**BSP**–$(CB[7])_3$, orange. Some resonances are unlabeled because of spectral overlap. H-15 proton signals in case of G and H spectra are at 1.64 ppm and thus are not shown in the picture. (For interpretation of the references to colour in this figure legend, the reader is referred to the web version of this article.)

nitrogen atoms simultaneously because of the strong electrostatic repulsion between strongly polarized carbonyl portals of neighboring CB[7] units (Scheme 1). It should be noted that most ^{1}H NMR signals of the both inclusion complexes are strongly broadened, showing that interaction between host and guest molecules possesses the dynamic character. This is probably due to the shuttling motion of CB[7] between the two binding sites taking place after the protonation of **BSP** molecule. Integration of the appropriate proton resonances of **BSP** in ^{1}H NMR spectra in the presence of 2 equivalents of CB[7] indicates that more than 80% of **BSP** is combined with CB[7] forming mainly the $(H^+)_2$–**BSP**–$(CB[7])_2$ complex and **BSP**–$(CB[7])_2$ complex as a minor component.

When the molar ratio of CB[7] to the guest exceeds three, the changes in the ^{1}H NMR spectra suggest that mixture of the [3] pseudorotaxanes is converted into one [4]pseudorotaxane by successive threading of three CB[7] macrocycles on the frame of **BSP** molecule (Fig. 3g, h). Compared with the free **BSP**, the aliphatic H_{13}, H_{14} and H_{15} protons on the central linker conduct direct shielding effects ($\Delta\delta H_{13}$ = −0.73 ppm, $\Delta\delta H_{14}$ = −0.73 ppm, $\Delta\delta H_{15}$ = −0.44 ppm and $\Delta\delta H_{16,17}$ = −0.35 ppm at 1:5 **BSP**/CB[7] ratio), indicating that CB[7] macrocycle resides over the tetramethyl propandiaminium moiety. The upfield chemical shifts for protons of styryl fragments ($\Delta\delta H_{5,6}$ = −0.65 ppm, $\Delta\delta H_b$ = −0.51 ppm and $\Delta\delta H_a$ = −0.13 ppm at 1:5 **BSP**/CB[7] ratio)

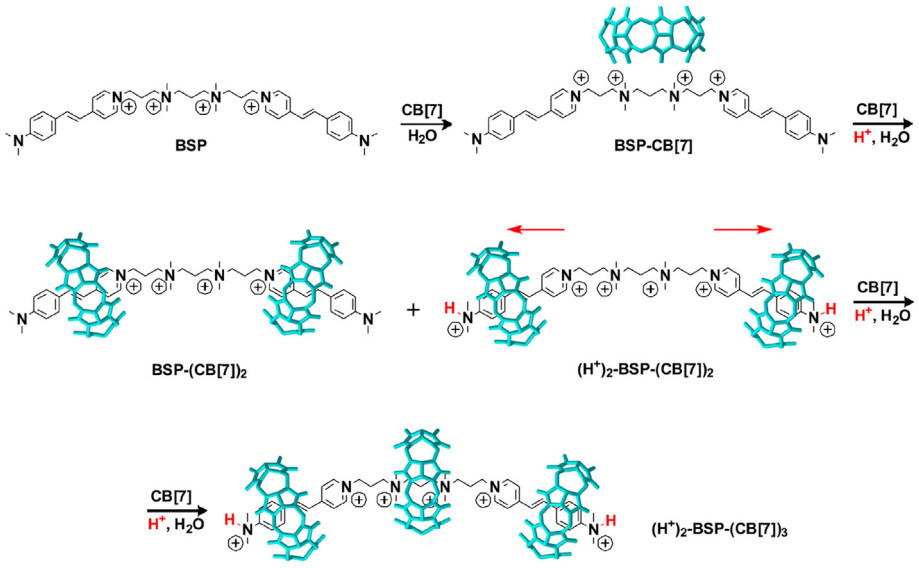

Scheme 1. Stepwise complex formation between **BSP** and CB[7] in aqueous solution.

were found, suggesting that these protons were encapsulated into CB[7] cavity. The proton signals for H_7, H_8, H_9 and H_{10} of pyridinium units, H_{11} and H_{12} of central aliphatic linker moved downfield ($\Delta\delta H_{7,8} = +0.66$ ppm, $\Delta\delta H_{9,10} = +0.51$ ppm, $\Delta\delta H_{11} = +0.35$ ppm and $\Delta\delta H_{12} = +0.75$ ppm at 1:5 **BSP**/CB[7] ratio), what is in accordance with their location outside of CB[7] cavity. In addition, the H_1 and H_2 protons of methyl groups and $H_{3,4}$ protons of phenyl ring became downfield shifted ($\Delta\delta H_{1,2} = +0.40$ ppm and $\Delta\delta H_{12} = +0.22$ ppm at 1:5 **BSP**/CB[7] ratio), that can be attributed to the protonation of amino groups. These spectroscopic results justify the contention, that CB[7] macrocycles in $(H^+)_2$–**BSP**–(CB[7])$_3$ complex would encircle three binding sites of **BSP** molecule as shown on Scheme 1: one of which is tetramethyl propandiaminium fragment of central linker and two other are dimethylamino styryl moieties.

Supporting evidence for the existence of $(H^+)_2$–**BSP**–(CB[7])$_3$ system comes from the diffusion ordered spectroscopy (DOSY) technique (Fig. S33). When 3.5 equiv. of CB[7] were added to the solution of **BSP**, only two species with logarithms of diffusion coefficients of $\log K^{dif}_{CB[7]} = -9.58$ and $\log K^{dif}_{complex} = -9.75$ associated with the free CB[7] and host–guest complex, respectively, were found. A detailed analysis of the signals corresponding to the host–guest complex showed that there are three CB[7] molecules per one ligand molecule that is in good agreement with the results of UV and ^{1}H NMR spectroscopy. Particularly, from Fig. S33 one can extract three types of signals relevant to CB[7], one of them can be attributed to free CB[7] and two others are associated with inclusion complexes between CB[7] and **BSP** molecules. The intensity of one of complex signal (assigned with the protons of dimethylamino styryl moieties) is twice as high as another one (assigned with the protons of the linker), that confirms our conclusion about the interaction of three CB[7] hosts with dye molecule in $(H^+)_2$–**BSP**–(CB[7])$_3$ complex.

The effect of host–guest interaction is also reflected in proton resonances for methylene groups linking the glycoluril units in CB[7]. Upon complexation with **BSP**, the doublet resonances of CB[7] at 4.14 and 5.69 ppm undergo splitting, indicating that oxygen portals of CB[7] are not in the same environments (Fig. S7). For example, in the case of exclusion complex **BSP**–CB[7] only one portal of CB[7] interacts with guest molecule. Another host portal is still remained free from any complexation (Scheme 1). Given complex configuration completely explains the observed splitting of the ^{1}H NMR resonances for CB[7] molecule. In contrast to this, no any splitting of proton signals have been observed for early reported (bis)styryl dyes [22], which form symmetrical exclusion complexes of the (dye)$_2$-CB[7] type by means of interaction of two dye molecules with both portals of CB[7]. The same arguments can be also made with respect to pseudorotaxane complexes.

Interestingly, when the CB[7]/**BSP** ratio exceeds 3, complex formation induces the appearance of a two sets of proton signals for CB[7] (Fig. S7g, h). One of them corresponds to the proton signals (doublets at 5.69 and 4.17 ppm and singlet at 5.45 ppm) observed at lower concentration of CB[7] in solution that were assigned to the location of host molecule at the aromatic fragments of **BSP**. The second set of proton signals (doublets at 5.75 and 4.33 ppm and singlet at 5.60 ppm) shifts downfield by about 0.10–0.20 ppm compared to the free CB[7]. Let us recall, according to the proton resonances for the **BSP** in the presence of 3 equiv. of CB[7] an inclusion complex $(H^+)_2$–**BSP**–(CB[7])$_3$ is formed, where two of three CB[7] macrocycles resides over the styrylpyridinium fragments whereas the other one encircles the central linker (Scheme 1). It is known that host–guest interaction effects on the charge distribution processes of the encapsulated guest molecules, modulating their chemical and physicochemical properties [9,10,53]. However, it was reasonable to assume that CB[7] itself may be influenced by guest molecules. In the case of $(H^+)_2$–**BSP**–(CB[7])$_3$ complex the both oxygen portals of central CB[7] are surrounded by four positively charged nitrogen atoms from pyridinium rings and propandiaminium moiety of **BSP**. Taking into account these facts, we suppose that donor properties of the carbonyl groups of CB[7] are decreased slightly due to its microenvironment and, as a result, the signals of neighboring protons undergo visible downfield shifts. Thus, it was concluded that second set of proton signals in Fig. S7g, h belong to the CB[7] macrocycle located over the central binding site of **BSP**.

We further decided to estimate the contribution to the change of ^{1}H NMR chemical shifts of dye molecule that make the complexation-induced protonation and host–guest interaction with CB[7] itself. For this purpose we studied these two processes by NMR spectroscopy separately. In the first step, we prepared a deuterated aqueous solution of di-protonated form of **BSP** (1.76×10^{-3} M **BSP** + 1.64×10^{-3} M $HClO_4$) and recorded its ^{1}H

NMR spectrum (Fig. S8). The addition of aqueous $HClO_4$ produced some changes in the resonances of the protons corresponding to the methyl groups and styrylpyridinium fragments by about 0.11–0.66 ppm. Specifically, the signal assigned to the $H_{3,4}$ protons of phenyl rings were noticeable shifted downfield ($\Delta\delta H_{3,4} = +0.66$ ppm), which clearly indicated that adjacent amine groups were protonated.

Next, we measured the ^{1}H NMR spectral changes of a solution of di-protonated form of **BSP** as the concentration of CB[7] was increased (Fig. S8). The binding mode of CB[7] with $(H^+)_2$–**BSP** was predicted using an analogy with data obtained from Fig. 3. Briefly, ^{1}H NMR spectroscopic experiments reveal that the presence of 0.5 or 1 equiv. of CB[7] leads to a splitting of the guest proton resonances into three separate sets. The first set of signals is similar to that of the unbounded guest and two other sets of signals reflect variable location of CB[7] wheels between ammonium and pyridinium moieties in the $(H^+)_2$–**BSP**–$(CB[7])_2$ complex (state I and II, Scheme S2). In state I (marked in green in Fig. S8), the $H_{3,4}$ and $H_{5,6}$ protons of aromatic rings ($\Delta\delta H_{3,4} = -0.34$ ppm and $\Delta\delta H_{5,6} = -0.87$ ppm at 1:0.5 $(H^+)_2$–**BSP**/CB[7] ratio) and the H_a and H_b protons of ethylene fragments ($\Delta\delta H_a = -0.55$ ppm and $\Delta\delta H_b = -0.68$ ppm at 1:0.5 $(H^+)_2$–**BSP**/CB[7] ratio) undergo significant downfield shifts, whereas the $H_{7,8}$ protons on the pyridinium rings ($\Delta\delta H_{7,8} = +0.32$ ppm at 1:0.5 $(H^+)_2$–**BSP**/CB[7] ratio) and the H_1 and H_2 protons of methyl groups ($\Delta\delta H_{1,2} = +0.14$ ppm at 1:0.5 $(H^+)_2$–**BSP**/CB[7] ratio) exhibits upfield shifts. Also, there was negligible change observed in the chemical shifts for the $H_{9,10}$ protons on the pyridinium rings and protons of the propandiaminium moiety ($\Delta\delta$ = 0.01–0.11 ppm). These observations indicate that styryl fragments of **BSP** were fully pulled inside the host cavity with the central linker staying outside. In contrast to this, in state II (marked in pink in Fig. S8) the CB[7] wheels are partly diverted from ammonium units to pyridinium units that supported by less expressed upfield shifts ($\Delta\delta H_{3,4} = -0.11$ ppm, $\Delta\delta H_{5,6} = -0.40$ ppm, $\Delta\delta H_a = -0.25$ ppm and $\Delta\delta H_b = -0.31$ ppm at 1:0.5 $(H^+)_2$–**BSP**/CB[7] ratio) and downfield shifts ($\Delta\delta H_{7,8} = +0.19$ ppm and $\Delta\delta H_{1,2} = +0.11$ ppm at 1:0.5 $(H^+)_2$–**BSP**/CB[7] ratio) for indicated proton signals. Upon addition of a slight excess of CB[7] (1.5 equiv.) to the $(H^+)_2$–**BSP** solution, the equilibrium is completely shifted towards complex with a CB[7] wheels docked nearby ammonium moieties (state I), as only one proton resonance is observed (Fig. S8). These findings confirm that CB[7] wheels in a $(H^+)_2$–**BSP**–$(CB[7])_2$ complex is mobile component and can perform shuttling motion. At higher concentration of CB[7] (2–2.5 equiv.) the proton resonances assigned to the complex $(H^+)_2$–**BSP**–$(CB[7])_3$ (marked orange in the Fig. S8) are appeared in the ^{1}H NMR spectra. Supporting this, the resonances of the protons $H_{3,4}$ and $H_{5,6}$ of aromatic rings ($\Delta\delta H_{3,4} = -0.45$ ppm and $\Delta\delta H_{5,6} = -0.91$ ppm at 1:2.5 $(H^+)_2$–**BSP**/CB[7] ratio) and H_a and H_b of ethylene fragments ($\Delta\delta H_a = -0.46$ ppm and $\Delta\delta H_b = -0.62$ ppm at 1:2.5 $(H^+)_2$–**BSP**/CB[7] ratio) as well as aliphatic protons H_{13}, H_{14}, H_{15}, $H_{16,17}$ of central linker ($\Delta\delta H_{13} = -0.84$ ppm, $\Delta\delta H_{14} = -0.77$ ppm, $\Delta\delta H_{15} = -0.61$ ppm and $\Delta\delta H_{16,17} = -0.36$ ppm at 1:2.5 $(H^+)_2$–**BSP**/CB[7] ratio) fall under shielding action of CB[7] cavity. At the same time, the H_1 and H_2 protons of methyl groups, $H_{7,8}$ and $H_{9,10}$ protons of pyridinium rings and H_{12} proton of aliphatic linker become downfield shifted ($\Delta\delta H_{1,2} = +0.12$ ppm, $\Delta\delta H_{7,8} = +0.42$ ppm, $\Delta\delta H_{9,10} = +0.26$ ppm and $\Delta\delta H_{12} = +0.66$ ppm at 1:2.5 $(H^+)_2$–**BSP**/CB[7] ratio), that was attributed to the deshielding effect of carbonyl groups of CB[7]. As far as the dye molecules were initially in the protonated form, we were not able to detect an exclusive **BSP**–CB[7] as well as inclusion **BSP**–$(CB[7])_2$ complexes that exists in aqueous solution at low concentration of CB[7] in the absence of $HClO_4$. Overall, obtained results are fully congruent with the conclusions that were done based on the ^{1}H NMR titration data of aqueous solution of unprotonated **BSP** with CB[7].

3.3. Electrospray ionization mass spectrometry

Additional support of the composition of the complexes of **BSP** with CB[7] was obtained from ESI-MS experiments. Complexes formed at the different **BSP**/CB[7] molar ratios were detected as multiply charged ions (see Table 1 and Figs. S34–S37). When the ratio of **BSP**: CB[7] is 1:1 the main complex observed at *m/z* 456.4 is [**BSP**–CB[7]]$^{4+}$. Increasing the amount of CB[7] up to a ratio of **BSP**: CB[7] = 1:5 causes the appearance of signals in the mass spectrum that correspond to complexes of unprotonated and monoprotonated dye, namely, [**BSP**–2CB[7]]$^{4+}$, [H–**BSP**–2CB[7]]$^{5+}$ and [H–**BSP**–3CB[7]]$^{5+}$. Thus, the ESI–MS data provide additional support for the stoichiometries of complexes derived from the optical measurements.

3.4. Complex formation

Here we summarize the information obtained from the UV and NMR spectroscopy and ESI-mass spectrometry and compare CB[7] binding with (bis)styrylpyridinium dye in different environment (aqueous and buffer solutions). In both cases host–guest interaction possesses multistage character. First, let us contemplate the scheme of complex formation between **BSP** and CB[7] molecules in aqueous solution (Scheme 1). For the sufficiently low CB[7] concentrations used in the titration experiments, the exclusion **BSP**–CB[7] complex driven only by the ion-dipole interactions between four positively charged nitrogen atoms of **BSP** and the one carbonyl portal of CB[7] would mainly dominate in the system, which is supported by the high association constant. Such associate has blue shifted long wavelength absorption band (Fig. 2a) and has less influence on the proton resonances in the ^{1}H NMR spectra of **BSP** because the protons of the dye are rather far from carbonyl groups of CB[7]. In addition, the signal at *m/z* 456.4 was assigned to 1:1 complex [**BSP**–CB[7]]$^{4+}$ (Fig. S35).

However, despite the high association constant for exclusion complex ($\log K_{11} = 6.4 \pm 0.4$ in aqueous solution), at higher concentration of CB[7] the equilibrium shifts toward the thermodynamically preferred inclusive complex **BSP**–$(CB[7])_2$ similar to [3]pseudorotaxane, in which the aromatic fragments of **BSP** are embedded inside the hydrophobic cavity of CB[7] and positively charged pyridinium nitrogens are placed closer to the negatively polarized carbonyl portals of CB[7]. This supramolecular association destabilizes the ICT state of dye molecule, leading to the facilitation of protonation of the aniline-type nitrogens. As a result, when the concentration of CB[7] is increased more than 1 equiv., the CB[7] macrocycles slides toward aniline ends of **BSP** and dimethylamino phenylethelene moieties also starts getting encapsulated, by forming a new [3]pseudorotaxane

Table 1
ESI–MS data for complexes between **BSP** and CB[7] in aqueous solution.

Ratio **BSP**/CB[7]	Assigned complex	Observed *m/z*	Calculated *m/z*[a]
1:0	[**BSP**–I]$^{3+}$	263.2	263.14
	[**BSP**–2I]$^{2+}$	458.1	458.16
1:1	[**BSP**–CB[7]]$^{4+}$	456.4	456.21
1:2	[**BSP**–CB[7]]$^{4+}$	456.4	456.21
	[H–**BSP**–2CB[7]]$^{5+}$	598.0	597.64
1:5	[H–**BSP**–2CB[7]]$^{5+}$	597.9	597.64
	[**BSP**–2CB[7]]$^{4+}$	747.2	746.80
	[H–**BSP**–3CB[7]]$^{5+}$	830.5	830.11

[a] Calculated *m/z* were obtained based on the monoisotopic masses of **BSP** (662.50 Da), CB[7] (1162.34 Da) and I (126.91 Da).

$(H^+)_2$–**BSP**–$(CB[7])_2$. Protonation-induced shuttling motion of CB[7] between the two stable binding sites of **BSP** is readily detected by NMR spectroscopy. Since exchange processes between all species are slow on the NMR time scale we could observe the two separate sets of proton signals corresponding to both CB[7]-based [3]pseudorotaxanes. Also protonation of the aniline-type nitrogens introduces substantial changes in the charge transfer character of the dye molecule, completely destabilizing the ICT state, thereafter absorption band is extremely blue-shifted by 144 nm (Fig. 1a).

The extended aliphatic chain with intruded nitrogen cations, which connects the two styrylpyridinium units, is one possible binding site for CB[7]. However, when CB[7] is located over the pyridinium rings in the **BSP**–$(CB[7])_2$ complex, it was impossible to occupy the central linker because of the strong electrostatic repulsion between neighboring oxygen portals of hosts. Protonation-induced sliding of CB[7] from pyridinium rings to the aniline ends leads to the situation when the central binding site becomes more favorable for interaction with CB[7]. Therefore, the final stage of complex formation is self-organization of a multicomponent complex $(H^+)_2$–**BSP**–$(CB[7])_3$, in which the aromatic fragments as well as the aliphatic chain are engulfed by three molecules of CB[7]. Sequential threading of the CB[7] wheels on the frame of dye molecules was evidenced by ESI-MS spectra, in which the signals at *m/z* 597.9, 747.2 and 830.5 could be clearly assigned to the complexes of $[H–\mathbf{BSP}–2CB[7]]^{5+}$, $[\mathbf{BSP}–2CB[7]]^{4+}$ and $[H–\mathbf{BSP}–3CB[7]]^{5+}$, respectively (Figs. S36 and S37). It should be noted there is also a number of examples of inclusion complexes like oligo/polypseudorotaxanes consisting of molecules with more than one recognition sites and CB[n] units [69–71].

The present results are compared with the binding mode of **BSP** with CB[7] in buffer solution (Scheme S1). The remarkable difference between host–guest interactions in aqueous and buffer solutions comes from the absence of protonation of aniline ends in the **BSP**–$(CB[7])_2$ complex due to maintaining the constant pH value of the solution. This distinguishing feature directly determines the different spectral properties observed for the complex **BSP**–$(CB[7])_3$, formed at the final stage of complex formation. In sharp contrast to the blue-shifted absorption band for protonated complex $(H^+)_2$–**BSP**–$(CB[7])_3$, the formation of non-protonated complex **BSP**–$(CB[7])_3$ is accompanied by the appearance of a new absorption band centered at 533 nm. This band is red-shifted relative to the long wavelength absorption band of free dye by 53 nm and complex **BSP**–$(CB[7])_2$ by 26 nm (Fig. 2b). In complex **BSP**–$(CB[7])_3$ hydrophobic moieties of the dye are located in a nonpolar inner cavity of CB[7]s, rather than in aqueous solution. Being located in the vicinity of the dimethylamino groups, the negatively polarized carbonyl portals of CB[7] enhance the donor ability of dimethylamino groups of dye molecule, thus stabilizing the ICT state and leading to the displacement of the long-wavelength absorption band to the red spectral region.

As seen, sliding motions of CB[7]s from pyridinium rings to the aniline ends of **BSP** molecule are present not only in aqueous solution but in the buffered one. However, the driving force inducing these processes is specific for each case. As far as aqueous solution is concerned, the major role belongs to the protonation of aryl amino groups, accompanied by the formation of complex **BSP**–$(CB[7])_2$. Sliding motions of CB[7]s in buffer solution arise from electrostatic repulsion between carbonyl portals of CB[7] encircled aliphatic chain and CB[7]s located over pyridinium rings in complex **BSP**–$(CB[7])_3$.

4. Conclusion

In summary, this work demonstrates the importance of microenvironment in respect of complex formation between pH-sensitive guests and host molecules and their chemical and spectral properties. We state that the composition and geometry of the formed complexes depend on the relative stoichiometry of dye and CB[7] molecules with exclusion one-to-one complex dominating at low **BSP**/CB[7] ratio and inclusion one-to-three complex dominating at high **BSP**/CB[7] ratio. Intermediate complexes are [2] pseudorotaxanes with variational location of CB[7] relative to the dye molecule. **BSP** + CB[7] system behaves as a molecular shuttle with two recognition sites for CB[7], namely, the pyridinium rings and aniline fragments. A sliding motion can be induced by concomitant protonation of aryl amino groups of dye molecules in aqueous solution in **BSP**–$(CB[7])_2$ complex or electrostatic repulsions of CB[7] macrocycles in **BSP**–$(CB[7])_3$ complex in buffered one. Stimuli-responsive shuttling of the CB[7] complexes reported here could hold promise as components of more complex molecular machines, fluorescent on/off switches and sensors and other photonic devices.

Acknowledgments

This work was financially supported by Russian Foundation for Basic Research grants 16-33-00748 Мол_а to E.Y.C. (absorption data), 16-03-00423 to Y.V.F. (fluorescence and ESI-MS data) and 15-03-04695 to A.S.P (NMR data). The authors thank Prof. L. Isaacs (University of Maryland, USA) for his friendly help and providing cucurbit[7]uril for our study.

Appendix A. Supplementary data

Supplementary data related to this article can be found at http://dx.doi.org/10.1016/j.dyepig.2016.04.013.

References

[1] Kathirgamanathan P, Surendrakumar S, Vanga RR, Ravichandran S, Antipan-Lara J, Ganeshamurugan S, et al. Arylvinylene phenanthroline derivatives for electron transport in blue organic light emitting diodes. Org Electron 2011;12:666–76.
[2] Gu J, Yulan W, Chen W-Q, Dong X-Z, Duan X-M, Kawata S. Carbazole-based 1D and 2D hemicyanines: synthesis, two-photon absorption properties and application for two-photon photopolymerization 3D lithography. New J Chem 2007;31:63–8.
[3] Koleva BB, Stoyanov S, Kolev T, Petkov I, Spiteller M. Structural elucidation, optical, magnetic and nonlinear optical properties of oxystyryl dyes. Spectrochim Acta A 2009;71:1857–64.
[4] Iwase Y, Kamada K, Ohta K, Kondo K. Synthesis and photophysical properties of new two-photon absorption chromophores containing a diacetylene moiety as the central π-bridge. J Mater Chem 2003;13:1575–81.
[5] Tulyakova E, Delbaere S, Fedorov Yu, Jonusauskas G, Moiseeva A, Fedorova O. Multimodal metal cation sensing with bis(macrocyclic) dye. Chem Eur J 2011;17:10752–62.
[6] Bozdemir OA, Guliyev R, Buyukcakir O, Selcuk S, Kolemen S, Gulseren G, et al. Selective manipulation of ICT and PET processes in styryl-bodipy derivatives: applications in molecular logic and fluorescence sensing of metal ions. J Am Chem Soc 2010;132:8029–36.
[7] Shen X, Jiang Q, Wang J, Dai L, Zou G, Wang ZG, et al. Visualization of the intracellular location and stability of DNA origami with a label-free fluorescent probe. Chem Commun 2012;48:11301–3.
[8] Garcia-Acosta B, Martines-Máñes R, Ros-Lis JV, Sancenón F, Soto J. Discrimination between ω-amino acids with chromogenic acyclic tripodal receptors functionalized with stilbazolium dyes. Tetrahedron Lett 2008;49:1997–2001.
[9] Dsouza RN, Pischel U, Nau WM. Fluorescent dyes and their supramolecular host/guest complexes with macrocycles in aqueous solution. Chem Rev 2011;111(12):7941–80.
[10] Arunkumar E, Forbes CC, Smith BD. Improving the properties of organic dyes by molecular encapsulation. Eur J Org Chem 2005:4051–9.
[11] Mock WL, Shih NY. Structure and selectivity in host-guest complexes of cucurbituril. J Org Chem 1986;51:4440–6.
[12] Lee JW, Samal S, Selvapalam N, Kim H-J, Kim K. Cucurbituril homologues and derivatives: new opportunities in supramolecular chemistry. Acc Chem Res 2003;36:621–30.
[13] Nau WM, Florea M, Assaf KI. Deep inside cucurbiturils: physical properties and volumes of their inner cavity determine the hydrophobic driving force for

host–guest complexation. Isr J Chem 2011;51:559–77.
[14] Márquez C, Nau WM. Polarizabilities inside molecular containers. Angew Chem Int Ed 2001;40:4387–90.
[15] Liu S, Ruspic C, Mukhopadhyay P, Chakrabarti S, Zavalij PY, Isaacs L. The cucurbit[n]uril family: prime components for self-sorting systems. J Am Chem Soc 2005;127:15959–67.
[16] Cao L, Sekutor M, Zavalij PY, Mlinaric-Majerski K, Glaser R, Isaacs L. Cucurbit [7]uril·guest pair with an attomolar dissociation constant. Angew Chem Int Ed 2014;53:988–93.
[17] Assaf KI, Nau WM. Cucurbiturils: from synthesis to high-affinity binding and catalysis. Chem Soc Rev 2015;44:394–418.
[18] Mohanty J, Nau WM. Ultrastable rhodamine with cucurbituril. Angew Chem Int Ed 2005;44:3750–4.
[19] Barooah N, Sundararajan M, Mohanty J, Bhasikuttan AC. Synergistic effect of intramolecular charge transfer toward supramolecular pKa shift in cucurbit[7] uril encapsulated coumarin dyes. J Phys Chem B 2014;118:7136–46.
[20] Sayed M, Sundararajan M, Mohanty J, Bhasikuttan AC, Pal H. Photophysical and quantum chemical studies on the interactions of oxazine-1 dye with cucurbituril macrocycles. J Phys Chem B 2015;119(7):3046–57.
[21] Zhang HY, Wang QC, Liu MH, Ma X, Tian H. Switchable V-type [2]pseudorotaxanes. Org Lett 2009;11:3234–7.
[22] Fedorova OA, Chernikova EY, Fedorov YV, Gulakova EN, Peregudov AS, Lyssenko KA, et al. Cucurbit[7]uril complexes of crown-ether derived styryl and (bis)styryl dyes. J Phys Chem B 2009;113:10149–58.
[23] Ivanov DA, Petrov NK, Nikitina EA, Basilevsky MV, Vedernikov AI, Gromov SP, et al. The 1:1 host–guest complexation between cucurbit[7]uril and styryl dye. J Phys Chem A 2011;115:4505–10.
[24] Li Z, Sun S, Liu F, Pang Y, Fan J, Song F, et al. Large fluorescence enhancement of a hemicyanine by supramolecular interaction with cucurbit[6]uril and its application as resettable logic gates. Dyes Pigments 2012;93:1401–7.
[25] Shaikh M, Mohanty J, Bhasikuttan AC, Uzunova VD, Nau WM, Pal H. Salt-induced guest relocation from a macrocyclic cavity into a biomolecular pocket: interplay between cucurbit[7]uril and albumin. Chem Commun 2008: 3681–3.
[26] Shaikh M, Choudhury SD, Mohanty J, Bhasikuttan AC, Pal H. Contrasting guest binding interaction of cucurbit[7-8]urils with neutral red dye: controlled exchange of multiple guests. Phys Chem Chem Phys 2010;12:7050–5.
[27] Shaikh M, Mohanty J, Singh PK, Nau WM, Pal H. Complexation of acridine orange by cucurbit[7]uril and beta-cyclodextrin: photophysical effects and pKa shifts. Photochem Photobiol Sci 2008;7:408–14.
[28] Bhasikuttan AC, Mohanty J, Nau WM, Pal H. Efficient fluorescence enhancement and cooperative binding of an organic dye in a supra-biomolecular host–protein assembly. Angew Chem Int Ed 2007;46:4120–2.
[29] Pischel U, Uzunova VD, Remóna P, Nau WM. Supramolecular logic with macrocyclic input and competitive reset. Chem Commun 2010;46:2635–7.
[30] Sindelar V, Parker SE, Kaifer AE. Inclusion of anthraquinone derivatives by the cucurbit[7]uril host. New J Chem 2007;31:725–8.
[31] Mohanty J, Bhasikuttan AC, Choudhury SD, Pal H. Noncovalent interaction of 5,10,15,20-tetrakis(4-N-methylpyridyl)porphyrin with cucurbit[7]uril: a supramolecular architecture. J Phys Chem B 2008;112(35):10782–5.
[32] Montes-Navajas P, Corma A, Garcia H. Complexation and fluorescence of tricyclic basic dyes encapsulated in cucurbiturils. Chemphyschem 2008;9: 713–20.
[33] Nau WM, Mohanty J. Taming fluorescent dyes with cucurbituril. Int J Photoenergy 2005;7:133–41.
[34] Koner AL, Nau WM. Cucurbituril encapsulation of fluorescent dyes. Supramol Chem 2007;19:55–66.
[35] Wang R, Yuan L, Macartney DH. A green to blue fluorescence switch of protonated 2-aminoanthracene upon inclusion in cucurbit[7]uril. Chem Commun 2005:5867–9.
[36] Wagner BD, Stojanovic N, Day AI, Blanch RJ. Host properties of cucurbit[7]uril: fluorescence enhancement of anilinonaphthalene sulfonates. J Phys Chem B 2003;107:10741–6.
[37] Mohanty J, Thakur N, Choudhury SD, Barooah N, Pal H, Bhasikuttan AC. Recognition-mediated light-up of thiazole orange with cucurbit[8]uril: exchange and release by chemical stimuli. J Phys Chem B 2012;116:130–5.
[38] Choudhury SD, Mohanty J, Upadhyaya HP, Bhasikuttan AC, Pal H. Photophysical studies on the noncovalent interaction of thioflavin T with cucurbit [n]uril macrocycles. J Phys Chem B 1891;2009:113–8.
[39] Barooah N, Mohanty J, Pal H, Bhasikuttan AC. Non-covalent interactions of coumarin dyes with cucurbit[7]uril macrocycle: modulation of ICT to TICT state conversion. Org Biomol Chem 2012;10:5055–62.
[40] Singh A, Yip W-T, Halterman RL. Fluorescence-on response via CB7 binding to viologen–dye pseudorotaxanes. Org Lett 2012;14:4046–9.
[41] Saleh N, Al-Soud YA, Al-Kaabi L, Ghosh I, Nau WM. A coumarin-based fluorescent PET sensor utilizing supramolecular pKa shifts. Tetrahedron Lett 2011;52:5249–54.
[42] Shaikh M, Choudhury SD, Mohanty J, Bhasikuttan AC, Nau WM, Pal H. Modulation of excited-state proton transfer of 2-(2′-hydroxyphenyl)benzimidazole in a macrocyclic cucurbit[7]uril host cavity: dual emission behavior and pK(a) shift. Chem Eur J 2009;15:12362–70.
[43] Basílio N, Laia CAT, Pina F. Excited-state proton transfer in confined medium. 4-methyl-7-hydroxyflavylium and β-naphthol incorporated in cucurbit[7]uril. J Phys Chem B 2015;119(6):2749–57.
[44] Barooah N, Mohanty J, Pal H, Bhasikuttan AC. Cucurbituril-induced supramolecular pKa shift in fluorescent dyes and its prospective applications. Proc Natl Acad Sci India Sect A Phys Sci 2014;84(1):1–17.
[45] Praetorius A, Bailey DM, Schwarzlose T, Nau WM. Design of a fluorescent dye for indicator displacement from cucurbiturils: a macrocycle-responsive fluorescent switch operating through a pKa shift. Org Lett 2008;10:4089–92.
[46] Barooah N, Mohanty J, Bhasikuttan AC. pH-mediated stoichiometric switching of cucurbit[8]uril–hoechst-33258 complexes. J Phys Chem B 2013;117: 13595–603.
[47] Zhang H, Liu L, Gao C, Sun R, Wang Q. Enhancing photostability of cyanine dye by cucurbituril encapsulation. Dyes Pigments 2012;94:266–70.
[48] Gadde S, Batchelaor EK, Weiss JP, Ling Y, Kaifer AE. Control of H- and J-aggregate formation via host-guest complexation using cucurbituril hosts. J Am Chem Soc 2008;130:17114–9.
[49] Xu Y, Panzner MJ, Li X, Youngs WJ, Pang Y. Host–guest assembly of squaraine dye in cucurbit[8]uril: its implication in fluorescent probe for mercury ions. Chem Commun 2010;46:4073–5.
[50] Halterman RL, Moore JL, Mannel LM. Disrupting aggregation of tethered rhodamine B dyads through inclusion in cucurbit[7]uril. J Org Chem 2008;73: 3266–9.
[51] Thangavel A, Elder IA, Sotiriou-Leventis C, Dawes R, Leventis N. Breaking aggregation and driving the keto-to-gem-diol equilibrium of the N,N′-dimethyl-2,6-diaza-9,10-anthraquinonediium dication to the keto form by intercalation in cucurbit[7]uril. J Org Chem 2013;78:8297–304.
[52] Pais VF, Carvalho EFA, Tome JPC, Pischel U. Supramolecular control of phthalocyanine dye aggregation. Supramol Chem 2014;26(9-9):642–7.
[53] Bhasikuttan AC, Pal H, Mohanty J. Cucurbit[n]uril based supramolecular assemblies: tunable physico-chemical properties and their prospects. Chem Commun 2011;47:9959–71.
[54] Masson E, Ling X, Joseph R, Kyeremeh-Mensah L, Lu X. Cucurbituril chemistry: a tale of supramolecular success. RSC Adv 2012;2:1213–47.
[55] Parvari G, Reany O, Keinan E. Applicable properties of cucurbiturils. Isr J Chem 2011;51:646–63.
[56] Yang Y-W. Towards biocompatible nanovalves based on mesoporous silica nanoparticles. Med Chem Commun 2011;2:1033–49.
[57] Mohanty J, Choudhury SD, Upadhyaya HP, Bhasikuttan AC, Pal H. Control of the supramolecular excimer formation of thioflavin T within a cucurbit[8]uril host: a fluorescence on/off mechanism. Chem Eur J 2009;15:5215–9.
[58] Wang R, Yuan L, Ihmels H, Macartney DH. Cucurbit[8]uril/cucurbit[7]uril controlled off/on fluorescence of the acridizinium and 9-aminoacridizinium cations in aqueous solution. Chem Eur J 2007;13:6468–73.
[59] Day A, Arnold AP, Blanch RJ, Snushall B. Controlling factors in the synthesis of cucurbituril and its homologues. J Org Chem 2001;66(24):8094–100.
[60] Huang W-H, Liu S, Isaacs L. Cucurbit[n]urils. Mod Supramol Chem 2008: 113–42.
[61] Tropcheva R, Lesev N, Danova S, Stoitsova S, Kaloyanova S. Novel cyanine dyes and homodimeric styryl dyes as fluorescent probes for assessment of lactic acid bacteria cell viability. J Photochem Photobiol B 2015;143:120–9.
[62] Kubin RF, Fletcher AN. Luminescence 1982;27:455–62.
[63] Marquez C, Hudgins RR, Nau WM. Mechanism of host–guest complexation by cucurbituril. J Am Chem Soc 2004;126:5806–16.
[64] Megyesi M, Biczók L, Jablonkai I. Highly sensitive fluorescence response to inclusion complex formation of berberine alkaloid with cucurbit[7]uril. J Phys Chem C 2008;112(9):3410–6.
[65] Ong W, Kaifer AE. Salt effects on the apparent stability of the Cucurbit[7] uril–methyl viologen inclusion complex. J Org Chem 2004;69:1383–5.
[66] Khan MSA, Heger D, Necas M, Sindelar V. Remarkable salt effect on stability of supramolecular complex between modified cucurbit[6]uril and methylviologen in aqueous media. J Phys Chem B 2009;113(32):11054–7.
[67] Tang H, Fuentealba D, Ko YH, Selvapalam N, Kim K, Bohne C. Guest binding dynamics with cucurbit[7]uril in the presence of cations. J Am Chem Soc 2011;133(50):20623–33.
[68] Chernikova E, Berdnikova D, Fedorov Y, Fedorova O, Peregudov A, Isaacs L. Self-assembly of a ternary architecture driven by cooperative Hg^{2+} ion binding between cucurbit[7]uril and crown ether macrocyclic hosts. Chem Commun 2012;48:7256–8.
[69] Liu Y, Shi J, Chen Y, Ke C-FA. Polymeric pseudorotaxane constructed from cucurbituril and aniline, and stabilization of its radical cation. Angew Chem Int Ed 2008;47:7293–6.
[70] Yin J, Chi C, Wu J. Efficient preparation of separable pseudo[n]rotaxanes by selective threading of oligoalkylammonium salts with cucurbit[7]uril. Chem Eur J 2009;15:6050–7.
[71] Cera L, Schalley CA. Stimuli-induced folding cascade of a linear oligomeric guest chain programmed through cucurbit[n]uril self-sorting (n = 6, 7, 8). Chem Sci 2014;5:2560–7.